Climate Dynamics (2001) 17: 433–444

G. Shaffer · S. M. Olsen

Sensitivity of the thermohaline circulation and climate to ocean exchanges in a simple coupled model

Received: 16 November 1999 / Accepted: 19 June 2000

Abstract A new simple, coupled climate model is presented and used to investigate the sensitivity of the thermohaline circulation and climate to ocean vertical and horizontal exchange. As formulated, the model highlights the role of thin, ocean surface layers in the communication between the atmosphere and the subsurface ocean. Model vertical exchange is considered to be an analogue to small-scale, diapycnal mixing and convection (when present) in the ocean. Model horizontal exchange is considered to be an analogue to the effects of the wind-driven circulation. For small vertical exchange in the ocean, the model exhibits only one steady-state solution: a relatively cold, mid-high-latitude climate associated with a weak, salinity-driven circulation (''off'' mode). For large vertical and horizontal exchange in the ocean, the model also exhibits only one steady-state solution: a relatively warm, mid-high-latitude climate associated with a strong, thermally-driven circulation (''on'' mode). For sufficiently weak horizontal exchange but large enough vertical exchange, both modes are possible stable, steady-state solutions. When model parameters are calibrated to fit tracer distributions of the modern ocean-atmosphere system, only the ''on'' mode is possible in this standard case. This suggests that the wind-driven circulation in consort with diapycnal mixing suppresses the ''off'' mode in the modern ocean-atmosphere system. Since both diapycnal mixing and the wind-driven circulation would be expected to increase in a cold climate with greater meridional temperature gradients and enhanced winds, vertical and horizontal exchange in the ocean are probably associated with strong negative feedbacks which tend to stabilize climate. These results point to the need to resolve ocean wind-driven circulation and to greatly improve the treatment of ocean diapycnal mixing in more complete models of the climate system.

G. Shaffer (✉) · S. M. Olsen
Danish Center for Earth System Science
Niels Bohr Institute for Astronomy, Physics and Geophysics
University of Copenhagen, Juliane Mariesvej 30,
2100 Copenhagen, Denmark
E-mail: gs@dcess.ku.dk

1 Introduction

The exchange of heat and fresh water between the atmosphere and the deep ocean is mediated by the <100 m thin, ocean surface layer. At low latitudes, atmospheric heating of this layer increases stratification at its base inhibiting vertical exchange. At high latitudes, atmospheric cooling of the layer decreases stratification, promoting vertical exchange, convection and deep water formation. The atmospheric fresh water cycle (net evaporation at low latitudes, net precipitation at high latitudes) opposes these effects on stratification via surface layer salinity but the thermal effect dominates in the modern ocean. One consequence of this is the partition of the ocean into the ''warm'', <1000 m deep, main ocean thermocline at low and mid latitudes (warm water sphere) and the ''cold'', deep and high-latitude ocean (cold water sphere). Considerable circulation and exchange exist within each of these spheres. This includes thermocline ventilation and deep recirculation to and from the Southern Ocean. It is useful to think of the thermohaline circulation as the net flow between these two ''spheres'', involving transformation of ''warm'' water to ''cold'' water and back again. In the modern ocean this flow carries about 20 Sv (1 Sverdrup is 10^6 m^3 s^{-1}) with the bulk of the deep water formation in the northern North Atlantic Ocean (Gordon 1986; Schmitz 1995).

Much attention has been focused on the ''cold'' branch of the thermohaline circulation but a deeper understanding of this circulation requires a close look at the ''warm'' branch as well. In the main thermocline, density is determined primarily by temperature and heat transport across isopycnal surfaces depends upon

small-scale, vertical (diapycnal) mixing. Such downward diffusive transport of heat absorbed by the ocean surface layer at low latitudes "balances" cooling from below in the deep upwelling of the "warm" branch of the thermohaline circulation (Munk 1966; Stommel and Arons 1960). A complementary pathway for transformation of cold water sphere to warm water sphere water involves deep upwelling in the Southern Ocean and diapycnal mixing/surface heating associated with this process (see Sect. 5). Thus, total transport in the thermohaline circulation is strongly, but not exclusively, controlled by the intensity of small-scale turbulence within the main ocean thermocline. Such strong sensitivity has been noted in ocean-only models (Bryan 1987; Zhang et al. 1999).

Two box, ocean-only models of the thermohaline circulation exhibit two stable steady-state solutions under a certain range of mixed boundary conditions (Stommel 1961). These solutions, the strong, thermally-driven, "on" mode and the weak, salinity-driven "off" mode, stem from the nonlinearity of this problem when surface forcing on temperature and salinity are decoupled. The Stommel (1961) model, coupled to a simple atmosphere model, still exhibits these two modes (Birchfield 1989; Marotzke and Stone 1995, referred to hereafter as MS). In such simple, coupled climate models, the "on" mode corresponds to a relatively warm, mid-high-latitude climate due to relatively large poleward, oceanic heat transport (but compensated in part by a relatively weak atmospheric heat transport). The "off" mode corresponds to a colder, mid-high-latitude climate due to weaker poleward, oceanic heat transport (but compensated in part by a stronger atmospheric heat transport). Thus, even such simple models can capture the essence of climate states found in much more complex coupled models (e.g. Manabe and Stouffer 1988).

In the MS model, the atmosphere is coupled directly to the deep ocean; this tacitly assumes infinite vertical mixing in the ocean while such mixing is rather weak in the real ocean. Also, in the MS model, the thermohaline circulation is the only mode of exchange between the warm and cold water spheres while wind-driven circulation gyres transport cold, fresh high-latitude water equatorward and warm, salty low-latitude water poleward in the real ocean. As discussed, the thermohaline circulation is likely to be quite sensitive to vertical and horizontal exchange. One important question for climate research is whether the "off" mode can exist for ocean exchange characterizing present and past climates.

Here we develop and apply perhaps the simplest possible coupled climate model suitable for the investigation of the effects of vertical and horizontal exchange in the ocean on the thermohaline circulation and climate. In Sect. 2 we develop the model and consider its steady-states. In Sect. 3 we use tracer distributions of the modern ocean-atmosphere system to calibrate free parameters of the model and discuss the nature of its solutions. In Sect. 4 we conduct sensitivity studies around this modern ocean-atmosphere analogue. Both vertical and horizontal exchange are found to strongly influence possible climate states as well as the climate within states possible. In particular, the "off" mode is found to be suppressed for model parameters calibrated to the modern ocean-atmosphere system. Finally in Sect. 5, on the basis of these results and other work, we discuss possible interactions between climate state and ocean exchange as well as the implications of such interactions for climate stability. Furthermore, we discuss our results in the context of other ocean and climate modelling work.

2 The simple coupled model

The one-hemisphere model consists of two atmospheric boxes and two deep ocean boxes separated in the vertical by two ocean surface layer boxes (Fig. 1). The model may be considered to be an extension of the MS model and much of the MS notation will be adopted here to facilitate comparison with the derivation and results of that model. The deep ocean boxes are well mixed and have depth D (taken to be 4000 m here). Subscript w and c refer to the low-latitude and mid-high-latitude sectors of equal area and volume, respectively, separated by 30° latitude.

Net radiation at the top of the atmosphere ($H^o_{w,c}$) is the sum of incoming, shortwave and outgoing, longwave radiation,

$$H^o_{w,c} = A_{w,c} - BT_{sw,sc} \quad (1)$$

where for low- and mid-high-latitudes, A_w and A_c are net incoming radiation for a surface temperature of 0 °C, T_{sw} and T_{sc} are sea

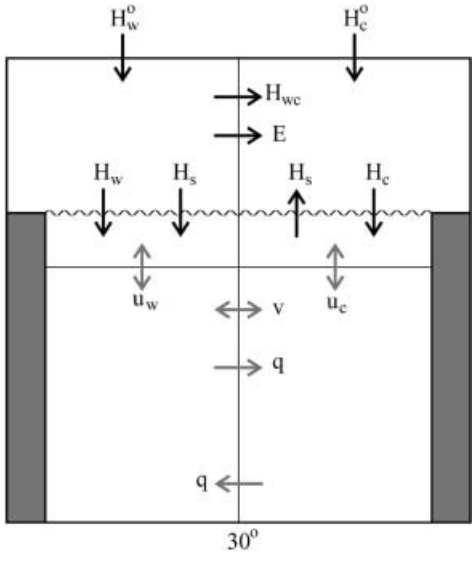

Fig. 1 The simple, coupled, ocean-atmosphere model including thin ocean surface layers. The one-hemisphere model is divided at 30° latitude into warm (w) low-latitude and cold (c) mid-high-latitude sectors of equal area and volume. Net radiation at the top-of-the-atmosphere $H^o_{w,c}$ is the sum of incoming shortwave and outgoing longwave radiation; H_{wc} and E are poleward eddy transports in the atmosphere of heat and water vapor, respectively; $H_{w,c}$ and H_s are heat and virtual salt exchanges at the ocean surface, respectively; $u_{w,c}$ are coefficients of vertical exchange between the surface and deep ocean and v is a coefficient of horizontal exchange between the deep ocean boxes. The thermohaline circulation intensity q is proportional to the density difference between the deep ocean boxes which depends on corresponding temperature and salinity differences

surface temperatures (and ocean surface layer temperatures; see below) and BT_{sw} and BT_{sc} are longwave fluxes caused by deviations of surface temperature from 0 °C. For simplicity, transports of heat (H_{wc}) and water vapor (E) across 30° in the atmosphere are assumed to be linearly related to sea surface temperature differences such that

$$H_{wc} = \chi(T_{sw} - T_{sc}),\ E = \gamma(T_{sw} - T_{sc}) \tag{2}$$

where χ and γ are atmospheric exchange coefficients and H_w and H_c are the heat exchanges across the low- and mid-high-latitude ocean surfaces. Virtual salt exchanges across these surfaces, H_s and $-H_s$, are $\rho_o \epsilon \epsilon_w^{-1} E S_o$ and $-\rho_o \epsilon \epsilon_w^{-1} E S_o$, respectively, where ρ_o is the water density, S_o is mean ocean salinity, ϵ is the ratio of ocean area to total ocean plus land area, and ϵ_w is the ratio of ocean area to catchment area, ($\epsilon \leq \epsilon_w \leq 1$); ϵ and ϵ_w are taken to be the same in both sectors for simplicity. The conversion of freshwater fluxes across the sea surface to salt fluxes in this way is an approximation which will be considered later. Heat exchanges between surface and deep ocean boxes at low- and mid-high-latitudes are assumed to be equal to $\rho_o c_p \epsilon D u_w (T_{sw} - T_{dw})$ and $\rho_o c_p \epsilon D u_c (T_{sc} - T_{dc})$, respectively, where c_p is the heat capacity, u_w and u_c are vertical exchange coefficients, and T_{dw} and T_{dc} are deep ocean temperatures. Corresponding salt exchanges are $\rho_o \epsilon D u_w (S_{sw} - S_{dw})$ and $\rho_o \epsilon D u_c (S_{sc} - S_{dc})$, where $S_{sw,sc}$ and $S_{dw,dc}$ are salinities in the surface layer and deep ocean, respectively. There is no net flow across 30° latitude in the surface layer (in the real ocean wind-driven Ekman transport tends to vanish at this latitude between tropical easterly and mid-latitude westerly winds).

The thermohaline circulation q is assumed to occur below the thin ocean surface layers and is taken to be proportional to the density difference between the deep ocean boxes, as in the original Stommel (1961) model. This density difference depends on corresponding temperature and salinity differences in the deep ocean through a linear equation of state such that

$$q = k[\alpha(T_{dw} - T_{dc}) - \beta(S_{dw} - S_{dc})] \tag{3}$$

where k is a flow parameter, α is the thermal expansion coefficient and β is the haline contraction coefficient. The circulation q is defined to be positive when density in the c deep box exceeds that in the w deep box. In addition to this circulation there is a horizontal exchange between the deep boxes associated with the exchange coefficient v. We interpret v mainly as the effect of the wind-driven, subtropical gyre circulation.

A key assumption of this simple model is that the heat and moisture capacities of the atmosphere and the heat and salt capacities of the ocean surface layer are negligible. Both the atmosphere and the surface layer are assumed to adjust "immediately" to changes in the deep ocean. Given typical ocean surface layer depths of 50–100 m, this approximation is valid for the long time scales (>10 years) of interest here. Then for each sector it follows that air-sea exchange of heat and water/salt can be determined as residuals of heat and water budgets for the atmosphere box and as residuals of heat and salt budgets for the ocean surface layer box whereby both residuals must match in each sector. This leads to the following relations

$$H_w = A_w - BT_{sw} - \chi(T_{sw} - T_{sc}) = \rho_o c_p \epsilon D u_w (T_{sw} - T_{dw}) \tag{4}$$

$$H_c = A_c - BT_{sc} + \chi(T_{sw} - T_{sc}) = \rho_o c_p \epsilon D u_c (T_{sc} - T_{dc}) \tag{5}$$

$$H_s = \rho_o S_o \frac{\epsilon}{\epsilon_w} \gamma (T_{sw} - T_{sc}) = \rho_o \epsilon D u_w (S_{sw} - S_{dw}) = -\rho_o \epsilon D u_c (S_{sc} - S_{dc})\ . \tag{6}$$

A more correct boundary condition for salinity in the problem may be found by treating explicitly the atmospheric fresh water flux entering the surface layer in the c sector and leaving the surface layer of the w sector. Then reconsideration of surface-layer salt budgets shows that S_o should be replaced by S_{sc} in Eq. (6). Significant errors due to our simplified formulation only arise if $u_{w,c}$ and v are very small (associated with ocean transports on the order of the atmospheric fresh water flux). Model results are not reliable for such low ocean exchanges which, however, are much less than required to explain observed ocean property distributions (see later). We retain the approximate boundary condition, Eq. (6), for simplicity and for the transparency of the analytical solutions which are possible when it is used.

Salt conservation in the deep ocean and the neglected salt capacity of the surface layer leads to

$$S_o = \tfrac{1}{2}(S_{dw} + S_{dc})\ . \tag{7}$$

For ocean surface layer depths of 50–100 m, the error associated with this approximation is several percent only.

The equations for heat and salt conservation in the deep boxes are

$$\frac{dT_{dw}}{dt} = u_w(T_{sw} - T_{dw}) - (|q| + v)(T_{dw} - T_{dc}) \tag{8}$$

$$\frac{dT_{dc}}{dt} = u_c(T_{sc} - T_{dc}) + (|q| + v)(T_{dw} - T_{dc}) \tag{9}$$

$$\frac{dS_{dw}}{dt} = u_w(S_{sw} - S_{dw}) - (|q| + v)(S_{dw} - S_{dc}) \tag{10}$$

$$\frac{dS_{dc}}{dt} = u_c(S_{sc} - S_{dc}) + (|q| + v)(S_{dw} - S_{dc})\ . \tag{11}$$

Together with diagnostic Eqs. (4)–(7), these equations can be reduced to three ordinary differential equations in the unknowns T_{dw}, T_{dc} and S_{dw} (or S_{dc}) or some combination of these unknowns. It is convenient to pose the problem in terms of T_{dm}, T and S, where T_{dm} is the mean temperature in the deep ocean $\frac{1}{2}(T_{dw} + T_{dc})$ and T and S are deep ocean temperature and salinity differences, $T_{dw} - T_{dc}$ and $S_{dw} - S_{dc}$. With these substitutions, the resulting model equations become

$$\frac{dT_{dm}}{dt} = (2\rho_o c_p \epsilon D)^{-1}(A_w + A_c - 2BT_{sm}) \tag{12}$$

$$\frac{dT}{dt} = \lambda(T_e - T_s) - 2vT - 2k|\alpha T - \beta S|T \tag{13}$$

$$\frac{dS}{dt} = \frac{2S_o\gamma}{\epsilon_w D} T_s - 2vS - 2k|\alpha T - \beta S|S \tag{14}$$

where T_{sm} is the mean surface temperature $\frac{1}{2}(T_{sw} + T_{sc})$, T_s is the surface temperature difference $T_{sw} - T_{sc}$, $T_e \equiv (A_w - A_c)/(2\chi + B)$ and $\lambda \equiv (2\chi + B)/(\epsilon\rho_o c_p D)$. Here T_e is the mean surface temperature difference between the two sectors in the absence of oceanic transports and the inverse of λ is the e-folding time of restoring the surface temperature difference to T_e after a perturbation in the absence of oceanic transports (see MS).

Together with expressions for T_{sm} and T_s (not shown) in terms of T_{dm}, T and S and the exchange and geometric parameters of the problem, Eqs. (12), (13) and (14) describe the time-dependent evolution of mean deep ocean temperature and temperature and salinity differences between the deep ocean boxes. The evolution of surface temperature, surface salinity difference and the thermohaline circulation can be diagnosed from the former three model variables.

From Eq. (6), the salinity difference $S_s = S_{sw} - S_{sc}$ in the ocean surface layer can be expressed as

$$S_s = \frac{(u_w + u_c)}{u_w u_c} \frac{S_o\gamma}{\epsilon_w D} T_s + S\ . \tag{15}$$

With a combined vertical exchange coefficient, u, defined as $2u_w u_c/(u_w + u_c)$, Eq. (15) simplifies to

$$S_s = \frac{2S_o\gamma}{u\epsilon_w D} T_s + S\ . \tag{16}$$

(Note that $u^{-1} = u_w^{-1} + u_c^{-1}$ where the terms are proportional to an overall, a low-latitude and a mid-high-latitude vertical mixing time,

respectively; the problem is analogous to two resistors connected in parallel). According to Eq. (16), the surface salinity difference blows up as $u \to 0$. With the more correct salinity boundary condition (see earlier), the surface salinity difference approaches $2S_o$ in that limit.

Our model reduces to the MS case as $u \to \infty$ and $v \to 0$. In this limit, deep and surface layer temperature and salinities converge (the deep ocean is coupled directly to the atmosphere) and the thermohaline circulation represents the only horizontal exchange in the ocean.

At steady-state, Eq. (12) leads to

$$T_{sm} = \frac{A_w + A_c}{2B} \quad . \tag{17}$$

This also follows directly from a condition of no net radiation at the top-of-the-atmosphere in a steady-state. Likewise, in a steady-state, net heat transport across the ocean surface must vanish such that $H_w + H_c = 0$. Then, from Eqs. (4) and (5) and the earlier definitions, we have

$$T_s = \frac{\lambda T_e(u_w + u_c) + 2u_w u_c T}{\lambda(u_w + u_c) + 2u_w u_c} \quad . \tag{18}$$

With the combined vertical exchange coefficient u this reduces to

$$T_s = \frac{\lambda T_e + uT}{u + \lambda} \quad . \tag{19}$$

With this result and Eq. (16), the steady-state salinity difference in the surface layer can be expressed as a linear function of T and S (not shown for brevity). Likewise, from the foregoing, steady-state expressions can also be derived for $T_{sw,sc}$ and $S_{dw,dc}$. For example, $T_{sc} = T_{sm} - \frac{1}{2}T_s$ which can be evaluated using Eq. (17) and (19). All variables of the problem except $T_{dw,dc}$ and $S_{sw,sc}$ can be expressed in terms of the combined vertical exchange coefficient u. To calculate the steady state value of $T_{dw,dc}$ (and thereby mean deep ocean temperature) and of $S_{sw,sc}$, either u_w or u_c must be specified in addition to u (see Eqs. 8–11).

Substitution of Eq. (19) into the steady-state versions of Eqs. (13) and (14) leads to two, time-independent, algebraic, nonlinear equations in T and S, which will be considered in detail later:

$$\frac{u}{(u+\lambda)}\lambda(T_e - T) - 2vT - 2k|\alpha T - \beta S|T = 0 \tag{20}$$

$$\frac{2S_o\gamma}{\epsilon_w D}\frac{(\lambda T_e + uT)}{(u+\lambda)} - 2vS - 2k|\alpha T - \beta S|S = 0 \quad . \tag{21}$$

As in the simple coupled models discussed in Sect. 1, stable "on" mode ($q > 0$) and "off" mode ($q < 0$) solutions can be found for this system, and when both of these solutions exist, a weak, unstable steady-state solution to the system with $q > 0$ is also found. We address in detail the structure of these steady-state solutions and their sensitivity to the oceanic exchange coefficients.

3 Structure of the steady-state solutions

For the analysis below it is useful to define a standard case, which should capture the current climate state, characterized by a vigorous "on" mode in the North Atlantic, as well as possible in our simple model context. We consider the Northern Hemisphere and take our model ocean to be an analogue of the North Atlantic. Since this ocean is about 60° wide, we take $\epsilon = \frac{1}{6}$. Since the North Atlantic has a large catchment area with runoff from North America and Asia, we take $\epsilon_w = \frac{1}{3}$ which corresponds to a catchment area 180° wide. In the context of our simple model, atmospheric heat transport also includes ocean heat transport in the North Pacific (as in MS). There is no deep water formation in the North Pacific in the modern ocean and most of the ocean heat transport across 30°N there (up to 1 PW) may be associated with the wind-driven circulation (Bryden et al. 1991). We introduce a separate v term in the North Atlantic to be able to address poleward heat and salt transport in this circulation. These transports affect the thermohaline circulation there and associated poleward heat transports.

The global distribution of annual-mean solar (shortwave) radiation at the top-of-the-atmosphere and the increase of the ice-free albedo with latitude can be estimated well using second-order Legendre polynomials (Hartmann 1994). Integrating the radiation, weighted by albedo, yields net incoming shortwave radiation of 309 W m^{-2} and 177 W m^{-2}, for the w and c sectors respectively, assuming the area north of 70°N to be ice-covered with constant albedo of 0.62. Observations indicate a value for B of about 2.2 W m^{-2} °C^{-1} (Graves et al. 1993). Given these values, a choice of a value for net outgoing radiation for a surface temperature of 0 °C leads to estimates of A_w and A_c and mean surface temperature T_{sm}. The choice of 209 W m^{-2} for this outgoing radiation agrees with observations (Graves et al. 1993) and yields values of A_w and A_c of 100 W m^{-2} and -32 W m^{-2}, respectively, and a realistic T_{sm} of 15.45 °C.

The remaining parameter values of our standard case are obtained by searching for an "on" mode solution of Eqs. (20) and (21) which matches the following observational constraints: a mean surface temperature difference of about 25 °C (our estimate from Hartmann 1994), warm water sphere-cold water sphere temperature and salinity differences of about 7.5 °C and 0.4 (our estimates from Levitus (1994) data with mean warm water sphere values calculated from the upper 800 m of the North Atlantic between 0 and 30°N), a thermohaline circulation of about 15 Sv (Gordon 1986; Schmitz 1995), a North Atlantic Ocean heat transport across 30°N of about 1 PW, the bulk of which is due to the thermohaline circulation (Hall and Bryden 1982), and an atmospheric water vapor transport across 30°N within the North Atlantic catchment area of about 0.25 Sv (Wijffels et al. 1992). The resulting, standard-case parameter values are given in Table 1. Standard values for u and v are 18 Sv and 5 Sv, respectively (these exchanges, and q later, have been scaled by multiplication with ocean sector volume, $\epsilon aD = 8.5 \cdot 10^{16}$ m^3 where a is the half hemisphere area; λ scaled in this way has a value of 159 Sv).

For the standard-case parameter values, we find the thermohaline circulation intensity, the surface temperature difference, the deep temperature difference, the deep salinity difference and the atmospheric water vapor transport across 30°N into the North Atlantic catchment area to be 15.09 Sv, 24.47 °C, 7.58 °C, 0.41 and 0.23 Sv, respectively. The surface temperature difference without North Atlantic heat transport, T_e, is 26.40 °C. Also, we find the atmospheric heat transport and the heat transports by the thermohaline circulation and by the horizontal exchange (attributed here to the

Table 1 Parameter definitions and standard case values

D	Ocean depth	4000 m
a	Half hemisphere area	$1.27 \cdot 10^{14}$ m^2
ϵ	Ocean to total area fraction	1/6
ϵ_w	Ocean to ocean catchment area fraction	1/3
S_o	Mean ocean salinity	35.22
ρ_o	Mean ocean water density	$1.0 \cdot 10^3$ kg m^{-3}
c_p	Specific heat capacity of water	$4.0 \cdot 10^3$ J kg^{-1} °C^{-1}
α	Thermal expansion coefficient	$2.0 \cdot 10^{-4}$ °C^{-1}
β	Haline contraction coefficient	$8.0 \cdot 10^{-4}$
A_w	Net incoming radiation for 0 °C in w sector	100 W m^{-2}
A_c	Net incoming radiation for 0 °C in c sector	−32 W m^{-2}
B	Sensitivity of LW radiation to surface temperature	2.2 W m^{-2} °C^{-1}
k	Thermohaline circulation flow parameter	$15 \cdot 10^{-8}$ s^{-1}
χ	Atmosphere exchange coefficient for heat	1.4 W m^{-2} °C^{-1}
γ	Atmosphere exchange coefficient for water vapor	$1.5 \cdot 10^{-10}$ m s^{-1} °C^{-1}
u	(Scaled) ocean vertical exchange coefficient	18 Sv
v	(Scaled) ocean horizontal exchange coefficient	5 Sv

wind-driven circulation) of the North Atlantic to be 4.35 PW, 0.46 PW and 0.15 PW, respectively. Although the heat transport due to the thermohaline circulation is somewhat low compared to observations (Hall and Bryden 1982), part of this transport in the real North Atlantic originates from the Southern Hemisphere. We can not deal with such cross hemisphere transport in our one hemisphere model.

To check the values of the ocean circulation and exchange parameters in the standard case solution, we solved for ocean Δ^{14}C distribution in our model and evaluated this solution for our standard case. For this, we assumed an atmospheric concentration of 0‰, a gas transfer velocity for CO_2 of $5.5 \cdot 10^{-5}$ m s^{-1} (Wanninkhof 1992) and we neglected the radioactive decay in the thin surface layers. The Δ^{14}C concentrations in the deep and surface ocean boxes depend on u_w and u_c. However, for standard-case parameter values and all combinations of u_w and u_c with $u = 18$ Sv, Δ^{14}C in both deep boxes lies in the range −70 to −75‰, in agreement with observed preanthropogenic values for the sub-surface North Atlantic (Shaffer and Sarmiento 1995).

For this "on" mode solution of our simple model it is reasonable to identify u_w with small-scale, diapycnal mixing and u_c with such mixing and, above all, convection. Indeed, in the c sector for standard-case parameters, water density in the surface layer exceeds that in the deep layer. This would motivate a choice of u_c to be considerably greater than u_w in this situation. One combination with $u = 18$ Sv would be u_w and u_c equal to 10 and 90 Sv, respectively. For these values, we find deep ocean temperatures, surface layer salinities and surface and deep layer Δ^{14}C which all agree quite well with North Atlantic observations, averaged as described already (in our calculations we used an S_o of 35.22, calculated for Levitus (1994) data from the North Atlantic Ocean). In the following, however, it will not be necessary to choose values for u_w and u_c: as shown above, only the combined vertical exchange coefficient u enters into the dynamics of the ocean and climate in the problem as posed. We will return to u_w and u_c in Sect. 5.

Figure 2 shows $T - S$ phase space plots of the steady-state solutions. The isoclines for time-independent T (Eq. 20; solid lines) and S (Eq. 21; dashed lines) are plotted for specific combinations of vertical and horizontal exchange. The T and S isoclines intersect at steady-state solution points. The thermohaline circulation intensity q is proportional to the distance from the solution points to the diagonal (dotted line) along a line normal to the diagonal. The diagonal marks $\alpha T = \beta S$ where temperature and salinity effects on this density difference cancel (see Eq. 3) and $q = 0$. Also shown are trajectories (thin lines) of the time-dependent solution for cases with $u_w = u_c$. Solution points to the left of the diagonal (thermally driven) are the strong, stable "on" mode (stable node) and a weak, unstable mode (saddle-point). The solution point to the right of the diagonal (salinity driven) is the weak, stable "off" mode (stable focus).

A comparison of Fig. 2a and b shows the effect of vertical exchange on the structure of model solutions in the absence of horizontal exchange. For all nonzero u, the T isocline intersects the diagonal at $(\alpha T_e, \alpha T_e)$: With $q = 0$, deep ocean temperatures would be equal to surface temperatures (Eqs. 8 and 9) and with $q, v = 0$, the surface temperature difference is T_e. As u decreases from $u \to \infty$ (Fig. 2a; MS case) to the vertical exchange of our standard case ($u = 18$ Sv; Fig. 2b), the deep ocean becomes less tightly coupled to the surface layer and thermohaline circulation acts to decrease the deep-ocean temperature difference. This is expressed in the figures by the rotation of the T isocline downward about its $q = 0$ pivot point. However, as this temperature difference decreases, so does the strength of the "on" mode; this allows the deep-ocean salinity difference to increase which further decreases the "on" mode strength. From Eq. (21), the position of the minimum of the S solution lies on the line $T_{min} = 2\alpha^{-1}\beta S_{min}$ for all u. Minimum T_{min} is found for $u \to \infty$ and is equal to $(\epsilon_w D k \alpha^2)^{-1}(4\beta S_o \gamma)$ which, for our standard-case parameters, has a value of 2.11 °C. As u decreases, T (and S) at the minimum of the S solution increases, approaching a maximum for $u \to 0$ of 7.47 °C for our standard-case parameters. Below some threshold for u, isoclines for T and S cease to

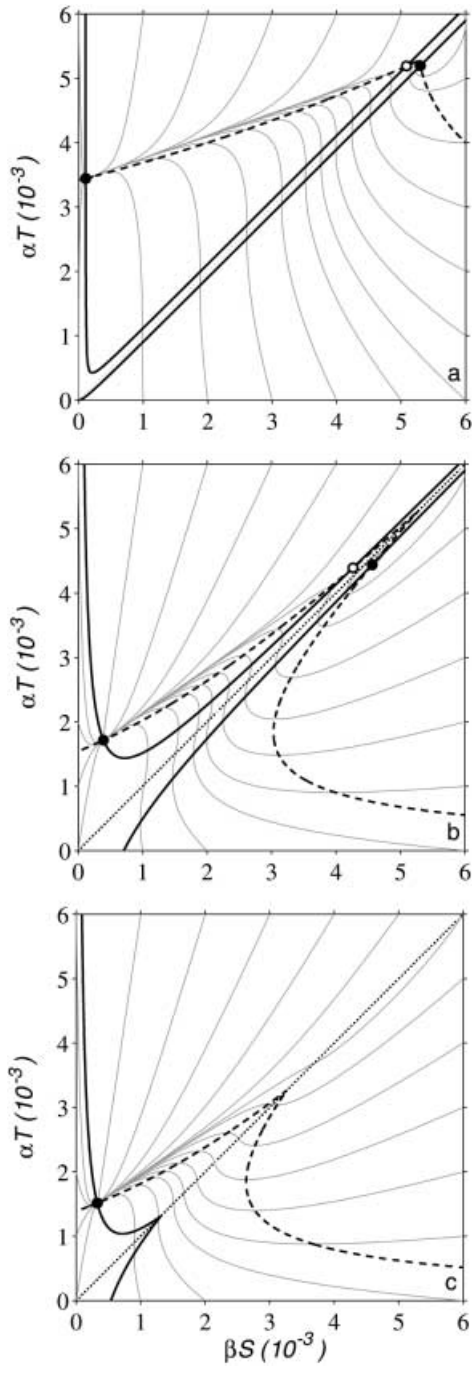

Fig. 2a–c Phase space plots of steady-state model equations for deep ocean temperature difference (T; *dashed thick lines*) and deep ocean salinity difference (S; *solid thick lines*) for several combinations of (scaled) vertical and horizontal exchange coefficients, u and v, and other parameters set to standard-case values (Table 1; $u \equiv 2u_w u_c/(u_w + u_c)$). To better illustrate their relative effects on deep ocean density difference, T and S have been multiplied by α and β, respectively. The *diagonal* (*dotted line*) marks $\alpha T = \beta S$ where $q = 0$. Steady-state model solutions are found at intersections of the T and S isoclines, marked by *filled* and *open dots* for stable and unstable steady states, respectively. Model results are shown for **a** $u \to \infty, v = 0$, **b** $u = 18$ Sv, $v = 0$ and **c** $u = 18$ Sv, $v = 5$ Sv (standard-case solution). Also shown are solution trajectories calculated numerically from the prognostic equations for T and S with u_w and u_c taken to be equal. In this special case the phase space of the time-dependent problem reduces to two dimensions (T, S) as in the general, steady-state phase space

intersect to the left of the diagonal and no "on" mode solution exists. For our standard-case parameters with $v = 0$, this threshold value for u is 5.22 Sv. Note that an "off" mode solution is found for all values of u for this case.

Figure 3 shows the variation with vertical exchange of the steady-state values of surface and deep ocean temperature and salinity differences and of thermohaline circulation intensity q. As u decreases for $v = 0$, these temperature and salinity differences become more decoupled from their surface layer forcing whereby surface differences of these properties become less constrained by the deep-ocean differences (Fig. 3a, b; thin lines). While the radiation balance combined with atmospheric transport puts a strong upper bound on the surface temperature difference in such a situation (see Eq. 19), the surface layer salinity difference is less constrained. In the absence of horizontal exchange, this salinity difference is inversely proportional to u (Eq. 16) and thus can become quite large for "weak" vertical exchange (see Fig. 3b). Even a "weak" u is large enough to communicate this "runaway" surface salinity difference to the deep ocean. Thus, the relative importance of salinity versus temperature forcing on the deep ocean shifts more toward salinity forcing as u becomes smaller. Since salinity forcing opposes the thermally driven, "on" mode, this mode eventually collapses for decreasing u (Fig. 3c; thin solid line). As u approaches (from above) its threshold for this collapse, T goes through a minimum and starts to increase (Fig. 3a). This final increase in T is due to a precipitous drop in q resulting in less exchange between the deep ocean boxes. The drop in q is associated with a rapid rise in S due to the still more rapid rise in surface layer salinity difference (Fig. 3b). For u below this threshhold, the only stable, steady-state solution to the problem is the salinity-driven, "off" mode (Fig. 3c, d).

A comparison of Fig. 2b and c shows the effect of horizontal exchange on the model solutions. Horizontal exchange reduces deep temperature and salinity differences and this reduction is communicated to the surface layer by vertical exchange. Due to this effect, for $v \neq 0$ the T isocline intersects the $q = 0$ diagonal at $(u\lambda + 2v(u + \lambda))^{-1} u\lambda\alpha T_e$ which for $u \ll \lambda$ approaches $(u + 2v)^{-1} u\alpha T_e$. Without horizontal exchange, the S isocline does not intersect the diagonal (Fig. 2b) since with $q, v = 0$ there is no model process which can balance the salinity forcing due to the atmospheric hydrological cycle. But for $v \neq 0$, it follows from Eq. (21) that the S isocline intersects the diagonal at a point which varies strongly with the inverse of v. These results show that, for sufficiently large u, there is a value of v at which both isoclines intersect the diagonal at the same point. For $u \to \infty$, this threshold value of v approaches $(\alpha\epsilon_w D)^{-1} \beta S_o \gamma$ which, for our standard-case parameters, has a value of 1.34 Sv; with these parameters and $u = 18$ Sv, the threshold value for v is 1.57 Sv. For horizontal exchange larger than the threshold value, the T and S isoclines do not intersect to the right of the

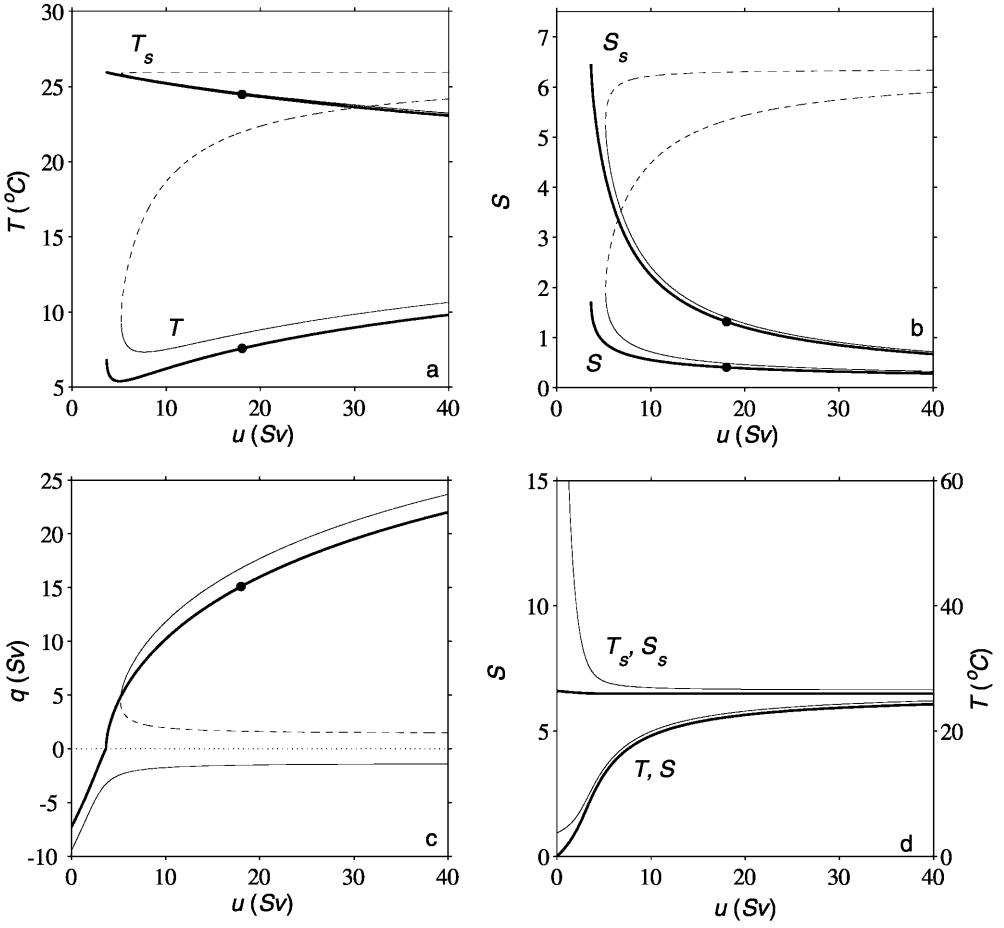

Fig. 3a–d Steady-state solutions as functions of vertical exchange coefficient u for **a** surface and deep ocean temperature differences, T_s and T and **b** surface and deep ocean salinity differences, S_s and S, both for thermally-driven solutions ($q > 0$), **c** thermohaline circulation intensity q, and **d** surface and deep ocean temperature differences (*thick lines*) and surface and deep salinity differences (*thin lines*) for salinity driven solutions ($q < 0$). Shown are stable (*solid lines*) and unstable (*dashed lines*), steady-state solutions for the cases with $v = 0$ (*thin lines* in **a**–**c**) and $v = 5$ Sv (*thick lines* in **a**–**c**), with all other parameters set to standard-case values. The *dots* mark the standard case, "on" mode solutions ($u = 18$ Sv, $v = 5$ Sv). The results in **d** are for the case with $v = 0$

diagonal and there is no "off" mode. In that case, which holds for our standard solution with $v = 5$ Sv (Fig. 2c), the "on" mode is the only stable, steady-state solution.

The elimination of the "off" mode for sufficiently strong horizontal and vertical exchange can be understood as follows: as v increases, deep-ocean temperature and salinity differences decrease. However, for sufficiently large u, the decrease in the deep-ocean temperature difference is "buffered" by exchange with the surface layer where the temperature difference is efficiently constrained by the radiation balance combined with the atmospheric transport ($\lambda \gg u, v$ in Eq. 19). In contrast, the surface salinity difference more readily decreases in response to a decrease in its deep ocean counterpart for sufficiently large u. As a result, the relative importance of temperature versus salinity forcing in the thermohaline circulation shifts more toward temperature forcing as v becomes larger. Since temperature forcing opposes the "off" mode, this mode will eventually be eliminated for increasing v and large enough u (Fig. 3c, thick line). For $v \to \infty$, this threshold value of u approaches $(\alpha\epsilon_w D)^{-1} 2\beta S_o \gamma$ which, for our standard-case parameters, has a value of 2.68 Sv. For u below this threshold – below 3.67 Sv with $v = 5$ Sv – the "runaway" surface salinity difference described will dominate and the only stable, steady-state solution is the "off" mode.

4 Sensitivity studies

In the analysis, three distinct regimes were identified for stable, steady-state solutions of the model. Figure 4 shows the distribution of these regimes for different combinations of vertical and horizontal exchange coefficients. In regime I, for small u and v, only the cold, "off" mode exists, while in regime III, for large u and v, only the warm, "on" mode exists. In regime II, for large enough u and small enough v, both stable, steady-state modes are possible model solutions.

The thermohaline circulation intensity q of the "on" mode (contours in Fig. 4a) increases rapidly as u increases from its threshold value at the boundary to regime I. In this range, q varies approximately as $u^{1/2}$ for u up to about 15 Sv. This dependency flattens out for increasing u until a maximum q is reached as $u \to \infty$ (MS case). For $v = 5$ Sv and standard-case parameters, this maximum "on" mode strength is 41.2 Sv. The strength of q for the "on" mode decreases with horizontal exchange since this exchange acts to decrease the thermal forcing of the mode. Thus, an increased wind-driven

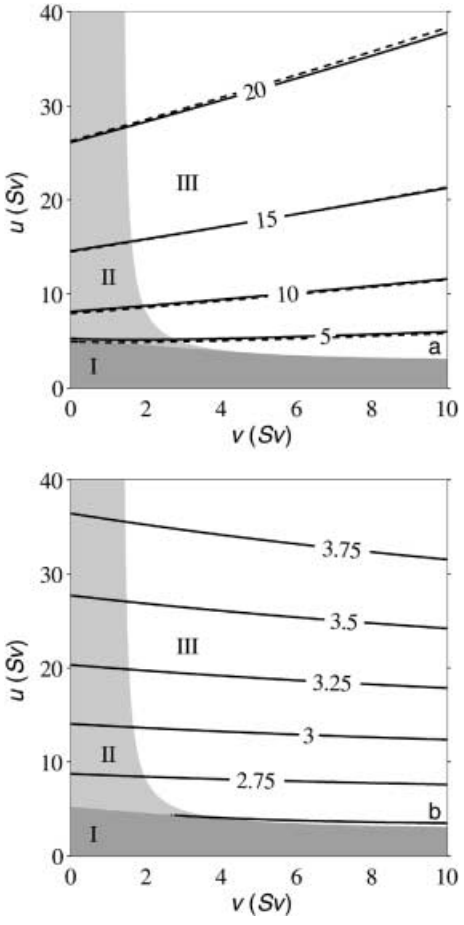

Fig. 4 **a** Thermohaline circulation intensity q in *Sv*, and **b** mid-high-latitude surface temperature T_{sc} in °C, for the "on" mode solution (stable, thermally driven), as functions of vertical and horizontal exchange coefficients, u and v, with all other parameters set to standard-case values. These results are plotted on a regime diagram whereby regimes I, II and III with *heavy*, *light*, and *no shading*, respectively, define the (u, v) parameter space in which only the "off" mode (stable, salinity driven), both "on" and "off" modes and only the "on" mode are found, respectively. Also shown are results for "on" mode q (*dashed lines* in **a**) for fixed atmospheric water vapor transport of 0.23 Sv to the North Atlantic catchment area

circulation would likely lead to a weaker "on" mode, thermohaline circulation. On the other hand, the weaker "on" mode in this case is more robust, in the sense of being farther removed from the regimes which permit the "off" mode solution (Fig. 4a).

For the "off" mode (not shown), q increases from zero at the boundary between regimes II and III as u and v decrease. This behavior reflects the greater sensitivity of salinity than of temperature to changes in ocean exchange for small u and v. For the virtual salt flux boundary condition, the "off" mode increases as $u \to 0$ (see Fig. 3c). But for the more correct boundary condition on salinity (see earlier), a maximum in "off" mode strength is found as u becomes very small and $q \to 0$ as $u \to 0$. In the real ocean, such very low values of vertical exchange need not be considered (see earlier).

Mid-high-latitude surface temperature T_{sc} associated with the "on" mode (contours in Fig. 4b) increases quite strongly with increasing vertical exchange and more weakly with increasing horizontal exchange. The temperature increase with increasing u is due mainly to increased poleward heat transport in a more vigorous thermohaline circulation. As v increases, increased poleward heat transport in the wind-driven circulation is opposed by decreased heat transport in the thermohaline circulation, explaining the weak temperature dependence on v. The dependency of T_{sc} on u flattens out for increasing u until a maximum is reached as $u \to \infty$. For $v = 5$ Sv and standard-case parameters, this maximum is 7.11 °C. For the "off" mode (not shown), T_{sc} is held quite constant in regime II to values only slightly lower than its "off" mode, upper limit, reached for $u \to \infty$ and $v = (\alpha \epsilon_w D)^{-1} \beta S_o \gamma$ (2.47 °C for standard-case parameters). The rather constant temperature as v decreases in this case is due to an approximate balance between reduced heat transport in horizontal mixing and increased heat transport in the "off" mode, thermohaline circulation. As $u \to 0$, the surface layer becomes isolated from the deep ocean and $T_{sc} \to T_{sm} - \frac{1}{2} T_e$ (2.26 °C for standard-case parameters).

In our simple climate model we adopted the eddy-moisture transport-thermohaline circulation (EMT) feedback (Nakamura et al. 1994), in the linear form of MS, whereby the poleward moisture transport in the atmosphere increases when the surface temperature difference increases. However, results from some coupled atmosphere-ocean GCM studies show decreased poleward moisture transport in the atmosphere in a cooler climate with increased surface temperature differences (Manabe and Stouffer 1994). This decrease was due to decreased carrying capacity of moisture in colder air. However, the relationship between this moisture transport and the meridional surface temperature gradient appears to be quite model-dependent (Rahmstorf and Ganopolski 1999). To test the sensitivity of our results to the EMT feedback, we also made simulations without this feedback whereby we fixed the atmospheric water vapor transport across 30°N into the North Atlantic catchment area to our standard-case value (0.23 Sv). Results for the "on" mode thermohaline circulation intensity with fixed water vapor transport (dashed lines in Fig. 4a) differ very little from those which include the EMT feedback. Likewise, our results for mid-high-latitude surface temperature are essentially unaffected by the exclusion of this feedback (not plotted in Fig. 4b since they are undistinguishable from results presented).

Figure 5a shows the dependence of the components of "on" mode, poleward heat transport across 30°N on ocean vertical and horizontal exchange. These heat transport components are due to the thermohaline circulation (thick lines), horizontal exchange (wind-driven circulation) in the North Atlantic (thin lines), and eddy transport of heat in the atmosphere (including wind-driven ocean transport in the Pacific; dashed lines). Of

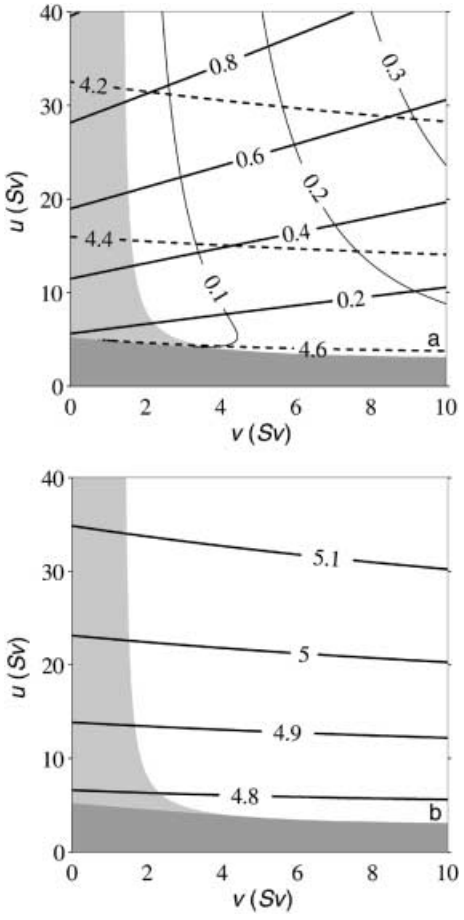

Fig. 5a, b Poleward heat transports across 30°N in PW for the "on" mode solution as functions of vertical and horizontal exchange coefficients, u and v, with all other parameters set to standard-case values. Shown are **a** heat transports due to the thermohaline circulation (*thick lines*), horizontal exchange (wind-driven circulation) in the North Atlantic Ocean (*thin lines*), and eddy transport of heat in the atmosphere (including wind-driven ocean transport in the Pacific Ocean; *dashed lines*) and **b** the total heat transport (the sum of the three components shown in **a**). Regimes I–III from Fig. 4 are indicated by *shading*

course, heat transport in the thermohaline circulation and in horizontal exchange are most sensitive to u and to v, respectively. While ocean heat transport increases with increasing u and v, the atmospheric eddy heat transport decreases as a consequence of more vigorous ocean exchange leading to decreasing surface temperature difference. Net ocean heat transport increases almost twice as much as the atmospheric heat transport decreases, leading to a net increase in total heat transport across 30°N (Fig. 5b). In the steady-state, this total heat transport must balance the net radiation to space north of 30°N which is $a(BT_{sc} - A_c)$. This is why isolines of total heat transport across 30°N in Fig. 5b parallel isolines of T_{sc} in Fig. 4b. For the "off" mode (not shown), total heat transport across 30°N is held quite constant in regime II to values only very slightly lower than its "off" mode upper limit (4.76 PW for standard-case parameters). As $u \to 0$, the surface layer becomes isolated from the deep ocean and there is no ocean heat transport. This case corresponds to maximum atmospheric (but minimum total) heat transport of $a\chi T_e$ (4.69 PW for standard case parameters).

Figure 6 shows the dependence of "on" mode, thermohaline circulation intensity q (solid lines) and mid-high-latitude surface temperature T_{sc} (dashed lines) on atmospheric exchange coefficients for heat and water vapor, χ and γ. Only the "on" mode was found for the range of χ and γ considered in the figure. According to our results, γ (and hence the poleward water vapor transport across 30°N) would have to more than double before the "off" mode would be a possible stable, steady-state solution for our standard-case parameters. Surface temperature is quite sensitive to χ since the bulk of the model heat transport takes place in the atmosphere (recall that this includes the wind-driven transport in the North Pacific). "On" mode q increases considerably as χ decreases. Increased poleward heat transport in the thermohaline circulation acts to dampen the effects of decreased atmospheric heat transport associated with a smaller χ. "On" mode q also increases for decreasing γ but in our model the thermohaline circulation is considerably more sensitive to changes in the eddy heat flux than to changes in the eddy water vapor flux.

5 Discussion

Here we presented a new simple, coupled climate model for one hemisphere and studied the nature and regimes of stable, steady-states of the model as functions of ocean vertical and horizontal exchange. The model features thin surface layers coupled to the atmosphere and by vertical exchange to a Stommel (1961) box model

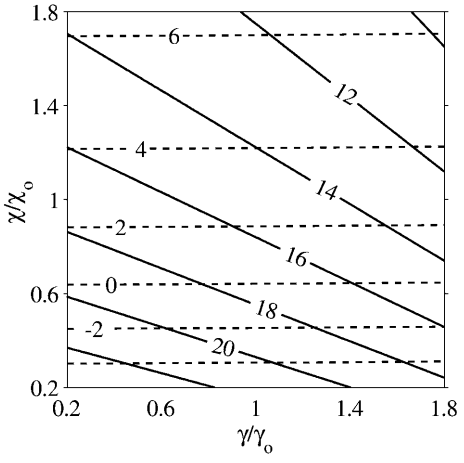

Fig. 6 Thermohaline circulation intensity q in Sv (*solid lines*) and mid-high-latitude surface temperature T_{sc} in °C (*dashed lines*) for the "on" mode solution as functions of atmospheric exchange coefficients for heat and water vapor, χ and γ, with all other parameters including u and v set to standard-case values. For the figure χ and γ have been scaled by their standard-case values, χ_o and γ_o (see Table 1)

of ocean thermohaline circulation, extended to include additional horizontal exchange. We consider this exchange to represent the effects of the wind-driven circulation. The warm deep box in the model is an analogue of the main ocean thermocline (warm water sphere) but for simplicity was taken to be equal in volume to the cold deep box (cold water sphere).

We demonstrated that the regimes and nature of possible stable, steady state solutions in this simple model depend only on a combined vertical exchange coefficient, u, rather than on the individual low- and mid-high-latitude exchange coefficients, u_w and u_c. It is reasonable to identify u_w and u_c with "background" small-scale, diapycnal mixing, complemented by convection when present. For the case with or without convection at high latitudes and only diapycnal mixing at low latitudes, one would have $u_w \leq u_c < \infty$ which from the definition of u implies $u_w \leq u < 2u_w$. Thus u would vary by at most a factor of two in the range of zero to infinite convection at high latitudes but would be quite sensitive to the level of diapycnal exchange. These results and our sensitivity analyses above suggest that changes in levels of diapycnal mixing in the ocean may have equal or greater effect on the strength of the thermohaline circulation and climate than changes in the intensity of high-latitude convection.

We identified a standard case for our model, intended to capture the current climate state with a vigorous "on" mode in the North Atlantic, by constraining the model with ocean and atmosphere temperature data and ocean salinity and ^{14}C data. The value of the horizontal exchange coefficient v deduced for this case exceeded by more than a factor of two a critical value above which only the "on" mode was possible in the model. Although v is one of the least well constrained model parameters, the standard value we choose for it is likely to be a conservative estimate: In the North Pacific, about twice as wide as the North Atlantic, estimates of poleward heat transport in the wind-driven circulation range up to 1 PW (Bryden et al. 1991). Our results suggest that wind-driven, ocean circulation may suppress the "off" mode in the present ocean-atmosphere system and may have suppressed this mode in the past. This may be the main reason why such a low-latitude sinking mode is usually not found in ocean general circulation models forced by wind stress and mixed boundary conditions (Bryan 1986; Marotzke and Willebrand 1991).

Both small-scale, diapycnal mixing and the wind-driven circulation may be expected to be sensitive to climate change. A turn to a colder climate would result in a larger meridional surface temperature gradient, an effect which would be strengthened by snow and ice albedo feedbacks. A larger temperature gradient leads to increased eddy activity in the atmosphere and enhanced poleward heat transport in the atmosphere. Increased eddy activity also promotes increased poleward transport of angular momentum resulting in stronger easterly winds in the tropics and stronger westerly winds at mid-latitudes (Bates 1999). This increased wind stress curl would force greater equatorward Sverdrup transport, a stronger subtropical ocean gyre and more effective horizontal exchange. As indicated by our model results, this would also lead to more poleward heat transport and warmer mid-high-latitudes (Fig. 4b) and, in addition, to a more robust "on" mode. Therefore, the wind-driven circulation may represent a negative feedback which tends to stabilize climate. In recent work with a complex, coupled ocean-atmosphere model, the wind-driven circulation was found to stabilize the "on" mode (Schiller et al. 1997).

The bulk of small-scale, diapycnal mixing in the ocean is ultimately forced by the action of tidal currents (e.g., through the generation and dissipation of internal tides in interaction with bottom topography) or by the surface winds (Munk and Wunsch 1998). The part of this mixing due to tides would be expected to be most important in the deep ocean and to be relatively insensitive to climate state. Our results indicate that "background" diapycnal mixing associated with tidal forcing would support at least a weaker "on" mode of the thermohaline circulation. Thus tidal mixing may have been an important player in climate stability over Earth history. As the ocean surface is approached from below, diapycnal mixing forced by the wind probably becomes more important. As argued, a colder climate would lead to stronger mean and variable winds. Together with weaker stratification expected in such a climate, increased wind forcing then would lead to greater diapycnal mixing. According to our results, this would force a stronger "on" mode, a weaker meridional surface temperature difference and a warmer climate at mid-high-latitudes (Fig. 4a, b). Therefore, diapycnal mixing would also represent a negative feedback which tends to stabilize climate. In a complex coupled, ocean-atmosphere model with flux corrections and prescribed vertical mixing coefficients, the "on" mode with vigorous deep water formation in the North Atlantic was found to be stable to large fresh water perturbations for sufficiently large vertical mixing (Manabe and Stouffer 1999). Our results point out the need to resolve well the wind-driven circulation and to greatly improve the treatment of ocean diapycnal exchange in complex, coupled models of the climate system.

Within the last decade, a number of studies have used three or four box ocean models in one hemisphere to address an ocean forced by mixed boundary conditions or a coupled ocean-atmosphere system (Birchfield 1989; Joyce 1991; Huang et al. 1992; Nakamura et al. 1994; Griffies and Tziperman 1995; Rivin and Tziperman 1997). Common to these models is that the thermohaline circulation passes through deep and "surface" boxes whereas the latter are typically identified with the main ocean thermocline (about 1000 m thick). Such model configurations allow the thermohaline circulation to be parameterized as an advection rather than effective horizontal mixing as in the Stommel (1961) model. On the other hand, such models are inherently flawed in a coupled ocean-atmosphere modelling context since

air-sea exchanges and atmospheric transports depend on surface properties (mainly SST), not on the mean properties of the main ocean thermocline or the deep ocean. Our model addresses this problem by considering surface boxes which correspond to surface mixed layers. These boxes are taken to be thin enough to neglect horizontal transport through them from wind-driven and thermohaline circulations and to neglect heat and salt storage in them for times greater than decades. Our approach is also suitable for considering other properties of the ocean-atmosphere system like CO_2 since air-sea exchange of dissolved gases depends on surface mixed layer concentrations which we model explicitly (see treatment of $\Delta^{14}C$). By calibration of model parameters to ocean and atmosphere data, we obtained realistic ocean surface layer (and deep ocean) temperatures and salinities.

Recent ocean modelling work has highlighted the role of Southern Ocean processes (and the role of diapycnal mixing) in determining ocean stratification and thermohaline circulation strength (Toggweiler and Samuels 1998; Gnanadesikan 1999; Vallis 1999). Transformation of cold water sphere to warm water sphere water occurs through some combination of diapycnal mixing in subsurface layers, supporting "upward", diapycnal flow there, and heating in the ocean surface layer of cold water sphere water upwelled into this layer (Walin 1982). In ocean models with lateral mixing along horizontal rather than isopycnal surfaces (e.g., Toggweiler and Samuels 1998), and in the presence of strongly sloping isopycnal surfaces (as in the Southern Ocean), such lateral mixing leads to large, spurious diapycnal mixing and associated spurious "upward" diapycnal flow (Veronis 1975). In such models, this effect would exaggerate the role of the Southern Ocean in controlling the ocean thermohaline circulation. Some ocean models show a rather strong, linear dependence of the strength of the Atlantic overturning circulation to the strength of Southern Ocean winds which force local upwelling (Toggweiler and Samuels 1995; Hasumi and Suginohara 1999). In these models with restoring boundary conditions, surface heating of cold, upwelled water in the surface Ekman layer would increase about linearly with the wind (and the equatorward flow in this layer forced by the wind). Accordingly, this would lead to a linear increase in ocean overturning. Thus, much of the increase in thermohaline circulation to increasing wind forcing in the Southern Ocean in such models may derive from inappropriate boundary conditions. These effects are likely to be much weaker in a coupled ocean-atmosphere system. Despite such shortcomings, work cited earlier has advanced our understanding of the role of both hemispheres and ocean geometry in the thermohaline circulation and climate, thereby providing guidance for future work.

Acknowledgements We thank two reviewers for helping us to improve our presentation. This work was supported by the Danish National Research Foundation and the Danish Natural Science Research Council.

References

Bates JR (1999) A dynamical stabilizer in the climate system: a mechanism suggested by a simple model. Tellus 51A: 349–372
Birchfield GE (1989) A coupled ocean-atmosphere climate model: temperature versus salinity effects on the thermohaline circulation. Clim Dyn 4: 57–71
Bryan F (1986) High-latitude salinity effeects and interhemispheric thermohaline circulations. Nature 323: 301–304
Bryan F (1987) Parameter sensitivity of primitive equation ocean general circulation models. J Phys Oceanogr 17: 970–985
Bryden HL, Roemmich DH, Church JA (1991) Ocean heat transport across 24°N in the Pacific. Deep-Sea Res 38: 297–324
Gnanadesikan A (1999) A simple predictive model for the structure of the oceanic pycnocline. Science 283: 2077–2079
Gordon A (1986) Interocean exchange of thermohaline water. J Geophys Res 91: 5037–5046
Graves CE, Lee W-H, North GR (1993) New parametrizations and sensitivities for simple climate models. J Geophys Res 98: 5025–5036
Griffies S, Tziperman E (1995) A linear thermohaline oscillator driven by stochastic atmospheric forcing. J Clim 8: 2440–2453
Hall MM, Bryden HL (1982) Direct estimates and mechanisms of ocean heat transport. Deep-Sea Res 29: 339–359
Hartmann DL (1994) Global physical climatology. Academic Press, San Diego, pp 411
Hasumi H, Suginohara N (1999) Atlantic deep circulation controlled by heating in the Southern Ocean. Geophys Res Lett 26: 1873–1876
Huang RX, Luyten JR, Stommel HM (1992) Multiple equilibrium states in combined thermal and saline circulation. J Phys Oceanogr 22: 231–246
Joyce TM (1991) Thermohaline catastrophe in a simple four-box model of the ocean climate. J Geophys Res 96: 20 393–20 402
Levitus S (1994) World ocean Atlas 1994 CD-ROM data set documentation. NODC Ocean Climate Laboratory, Washington, DC., Internal Rep 13
Manabe S, Stouffer RJ (1988) Two stable equilibria of a coupled ocean-atmosphere model. J Clim 1: 841–866
Manabe S, Stouffer RJ (1994) Multiple-century response of a coupled ocean-atmosphere model to an increase of atmospheric carbon dioxide. J Clim 7: 5–23
Manabe S, Stouffer RJ (1999) Are two modes of thermohaline circulation stable? Tellus 51A: 400–411
Marotzke J, Stone PH (1995) Atmospheric transports, the thermohaline circulation, and flux adjustments in a simple coupled model. J Phys Oceanogr 25: 1350–1364
Marotzke J, Willebrand J (1991) Multiple equilibria of the global thermohaline circulation. J Phys Oceanogr 21: 1372–1385
Munk WH (1966) Abyssal recipes. Deep-Sea Res 13: 707–730
Munk WH, Wunsch C (1998) Abyssal recipes II: energetics of tidal and wind mixing. Deep-Sea Res 45: 1977–2010
Nakamura M, Stone PH, Marotzke J (1994) Destabilization of the thermohaline circulation by atmospheric eddy transports. J Clim 7: 1870–1882
Rahmstorf S, Ganopolski A (1999) Long term global warming scenarios computed with an efficient coupled climate model. Clim Change 43: 353–367
Rivin I, Tziperman E (1997) Linear versus self-sustained interdecadal thermohaline variability in a coupled box model. J Phys Oceanogr 27: 1216–1232
Schiller A, Mikolajewicz U, Voss R (1997) The stability of the North Atlantic thermohaline circulation in a coupled ocean-atmosphere general circulation model. Clim Dyn 13: 325–347
Schmitz WJ Jr (1995) On the inter basin-scale thermohaline circulation. Rev Geophys 33: 151–173
Shaffer G, Sarmiento JL (1995) Biogeochemical cycling in the global ocean: 1. A new analytical model with continuous vertical resolution and high latitude dynamics. J Geophys Res 100: 2659–2672

Stommel H (1961) Thermohaline convection with two stable regimes of flow. Tellus 13: 224–230

Stommel H, Arons AB (1960) On the abyssal circulation of the worlds oceans. I. Stationary planetary flow patterns on a sphere. Deep-Sea Res 6: 140–154

Toggweiler JR, Samuels B (1995) Effect of Drake Passage on the global thermohaline circulation. Deep-Sea Res 42: 477–500

Toggweiler JR, Samuels B (1998) On the ocean's large-scale circulation near the limit of no vertical mixing. J Phys Oceanogr 28: 1832–1852

Vallis GK (1999) Large-scale circulation and production of stratification: effects of wind, geometry and diffusion. J Phys Oceanogr (in Press)

Veronis G (1975) The role of models in tracer studies. In: Reid RO, Robinson AR, Bryan K (eds) Numerical models of ocean circulation. National Academy of Science, Washington, DC, pp 133–146

Walin G (1982) On the relation between sea-surface heat flow and thermal circulation in the ocean. Tellus 4: 187–195

Wanninkhof R (1992) Relationship between wind speed and gas exchange over the ocean. J Geophys Res 97: 7373–7382

Wijffels SE, Schmitt RW, Bryden HL, Stigebrandt A (1992) Transport of freshwater by oceans. J Phys Oceanogr 22: 155–162

Zhang J, Schmitt RW, Huang RX (1999) The relative influence of diapycnal mixing and hydrological forcing on the stability of the thermohaline circulation. J Phys Oceanogr 29: 1096–1108